nature geoscience

SUPPLEMENTARY INFORMATION

DOI: 10.1038/NGEO1017

Miocene drainage reversal of the Amazon River driven by plate-mantle interaction.

Shephard, G.E., Müller, R.D., Liu, L., Gurnis, M.

Supplementary Figures

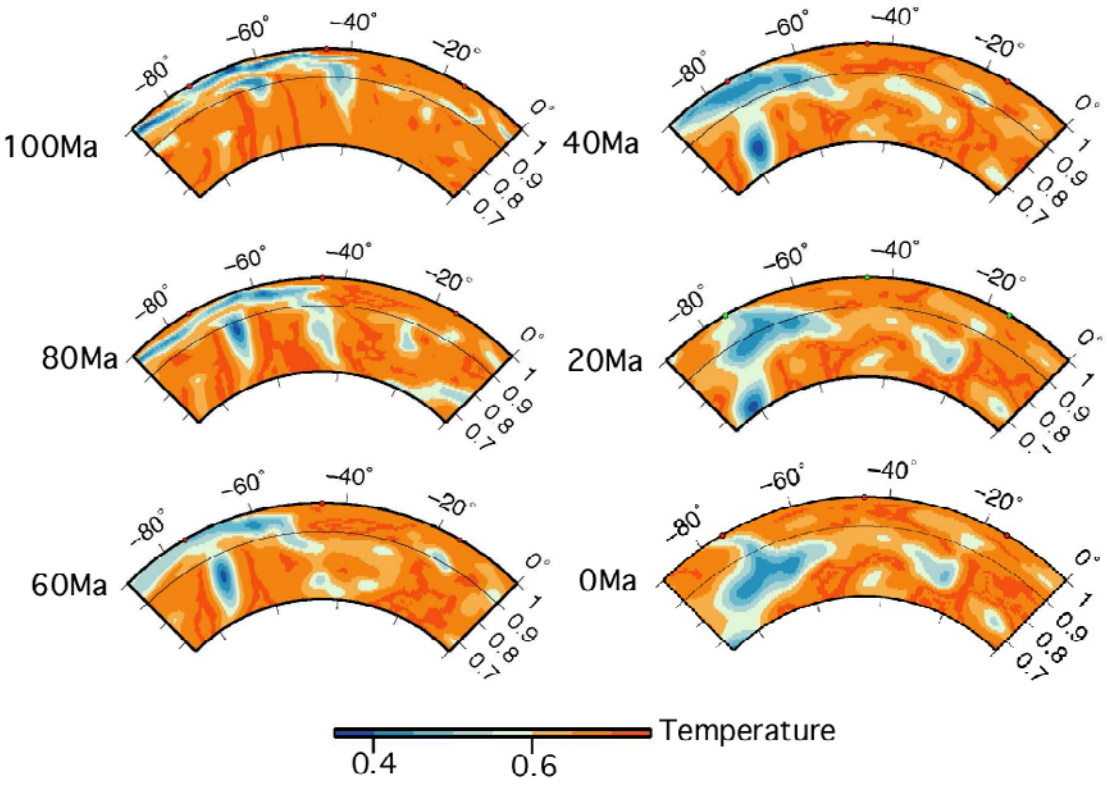

SOM Figure 1. Non-dimensional model mantle temperature cross-sections though the equator from 100 Ma to present for our best-fit model. Blue colours represent negative thermal anomalies (subducted slabs), whereas dark orange colours represent positive thermal anomalies (ambient mantle is light orange).

DOI: 10.1038/NGEO1017

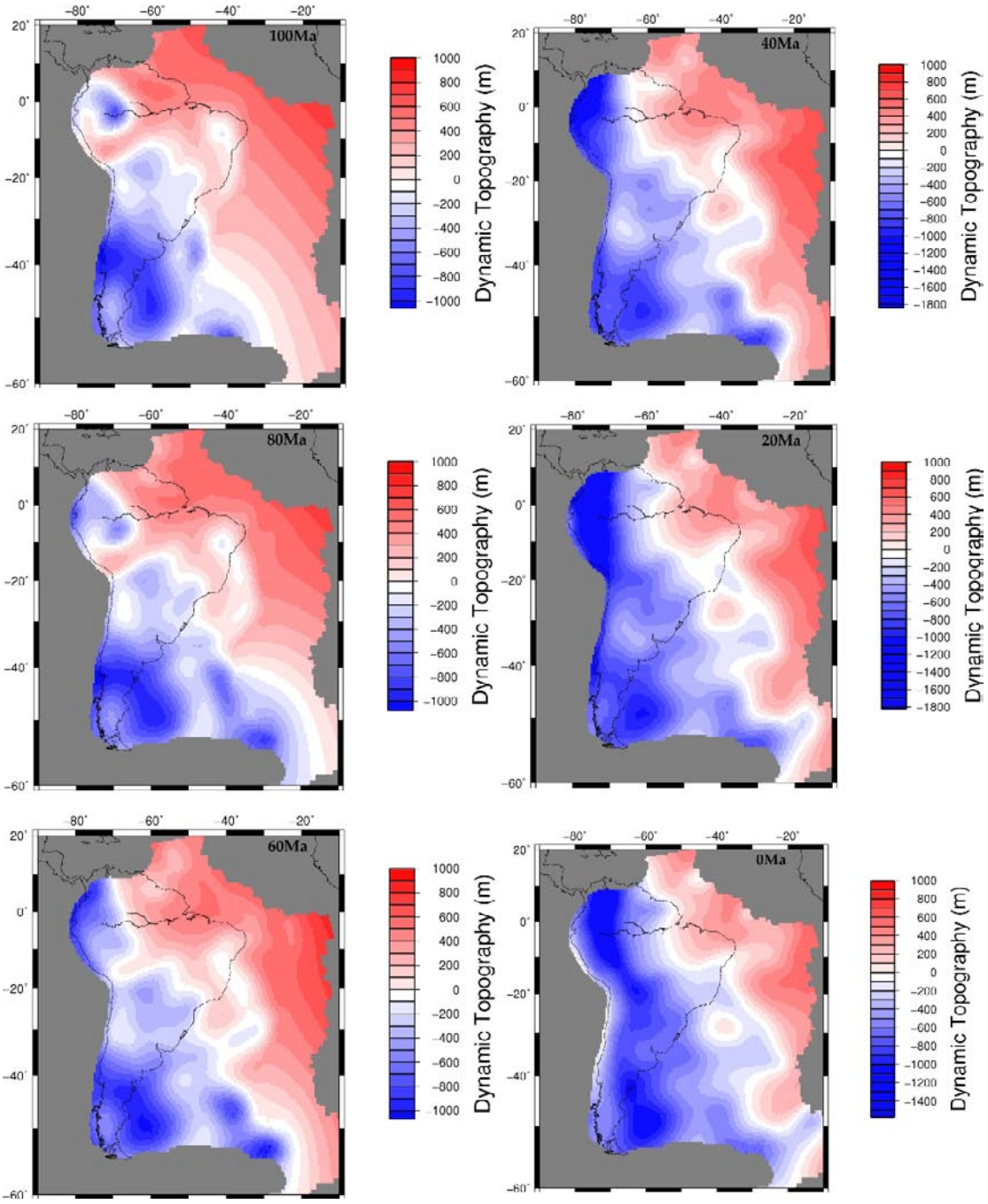

SOM Figure 2. Absolute surface dynamic topography since 100 Ma for our best-fit model. The blue indicates negative dynamic topography whereas the red indicates positive dynamic topography. Note, the fixed colour palette between ±1000 m but variable maximum and minimum values for each image. Grey areas indicate areas outside of the modeled domain.

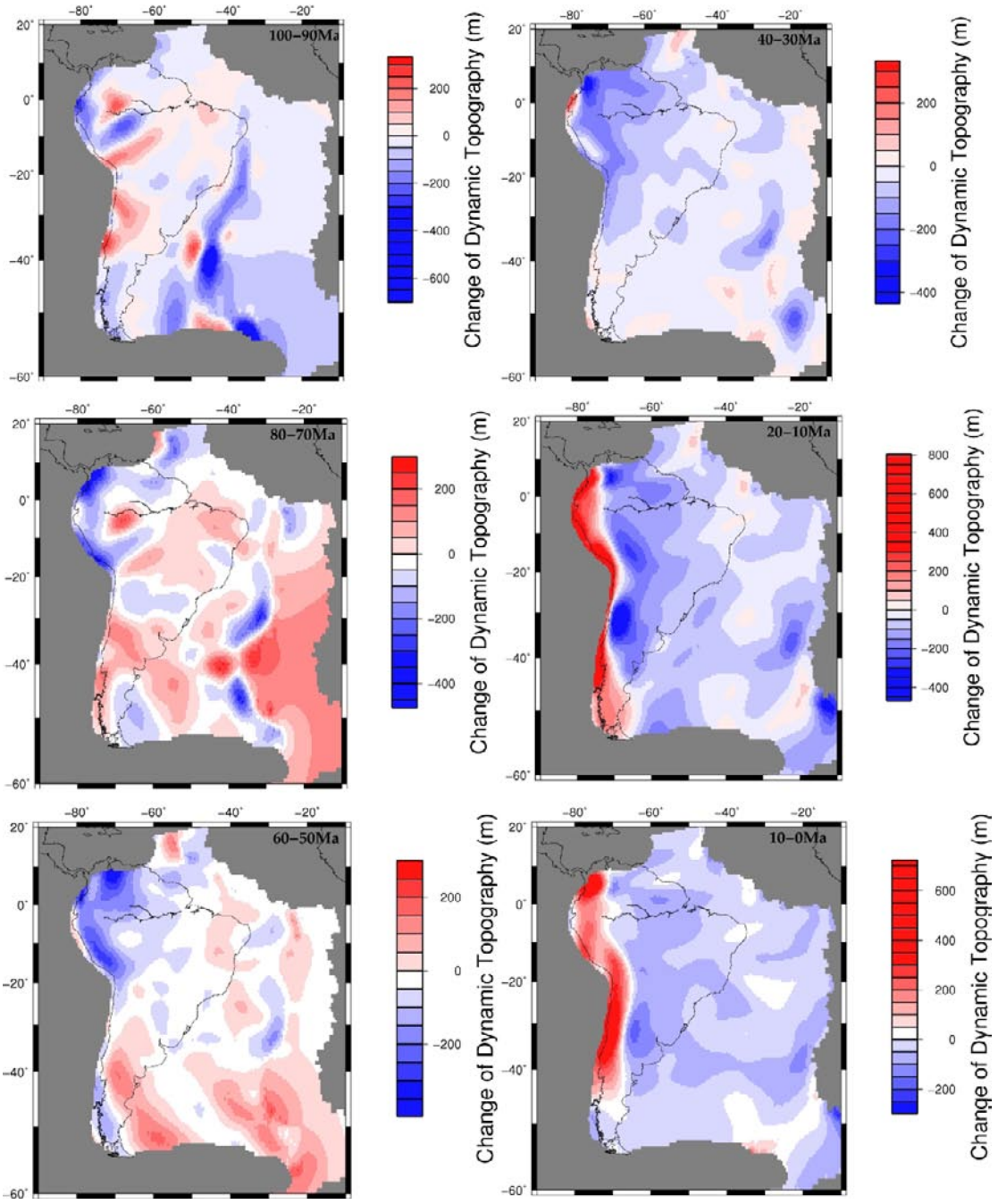

SOM Figure 3. Change in surface dynamic topography since 60 Ma in a fixed South America reference frame for six tectonic stages for our best fit model. Red indicates uplift, whereas blue indicates subsidence. Note, the fixed colour palette between ±300 m, but variable maximum and minimum values for each image.

DOI: 10.1038/NGEO1017

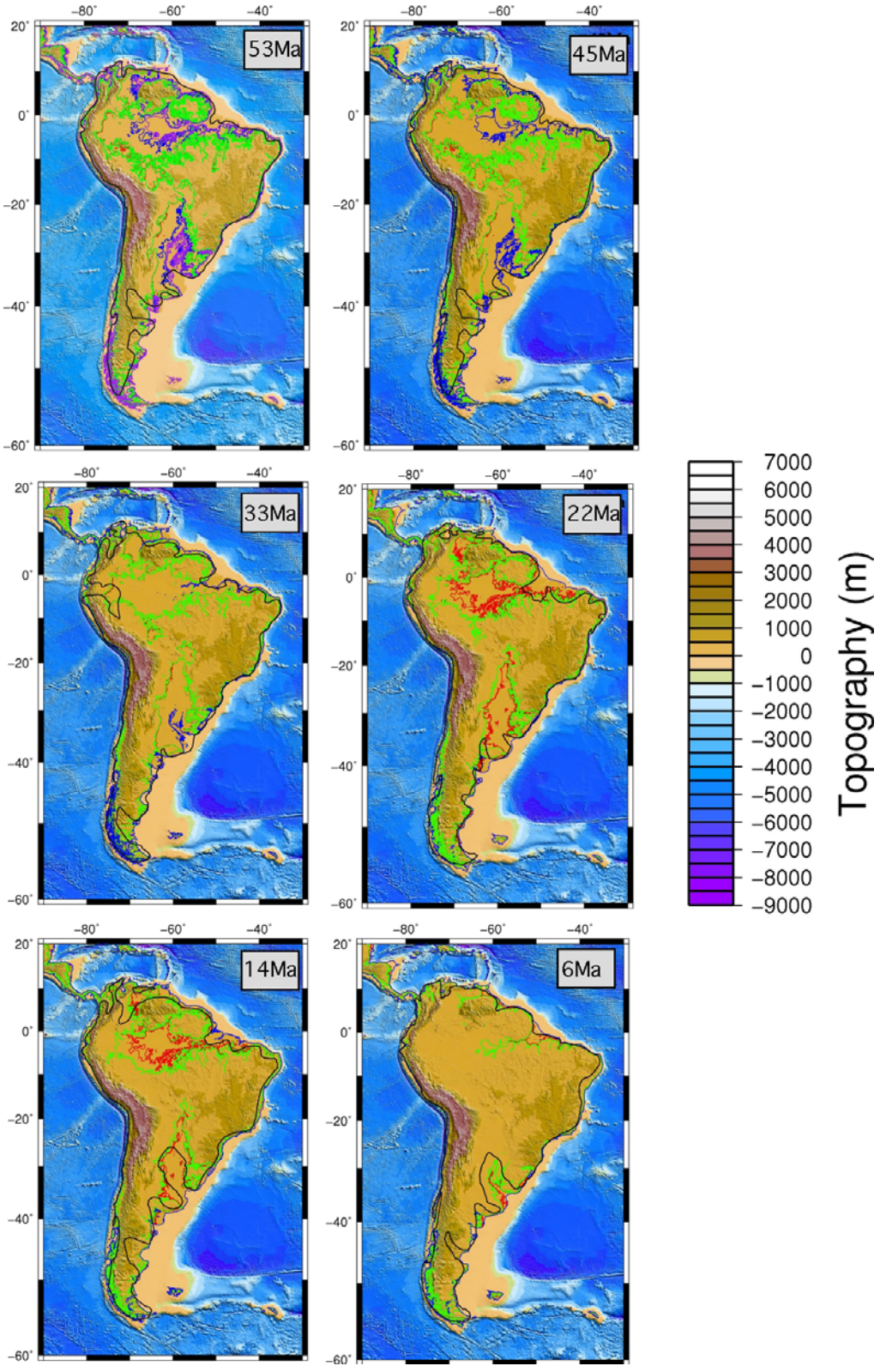

SOM Figure 4. Inundation maps of South America using present-day topography (ETOPO2) and inundating with three sea level curves to produced "predicted" palaeo-

coastlines; red showing Haq *et al.* (1987), green Haq and Al-Qahtani (2005) and blue, Miller *et al.* (2005). We decided to utilise the Haq *et al.* (1987) sea-level curve as we believe it to best represent global trends. The Miller *et al. (*2005) sea-level curve is not suitable because this sea-level curve is based solely on the New Jersey margin where dynamic subsidence is known to have affected relative sea level (Spasojevic *et al.,* 2008). This curve underestimates the late Paleogene and Neogene sea-level drop, which has been discussed previously (Müller *et al.,* 2008, Science), resulting from margin tectonic subsidence while global sea level dropped. Similarly, the Haq and Al-Qahtani (2005) curve is mainly based on the Arabian platform, which not-well understood in terms of dynamic topography through time. For comparison, the black outline shows "observed" palaeo-coastlines as derived by Golonka *et al*. (2006), based on terrestrial versus marine facies mapping. Note the excess inundation across the central and eastern basins. We interpret the difference between observed and predicted coastlines to be indicative of a significant long-wavelength change in topography i.e. broad subsidence.

DOI: 10.1038/NGEO1017

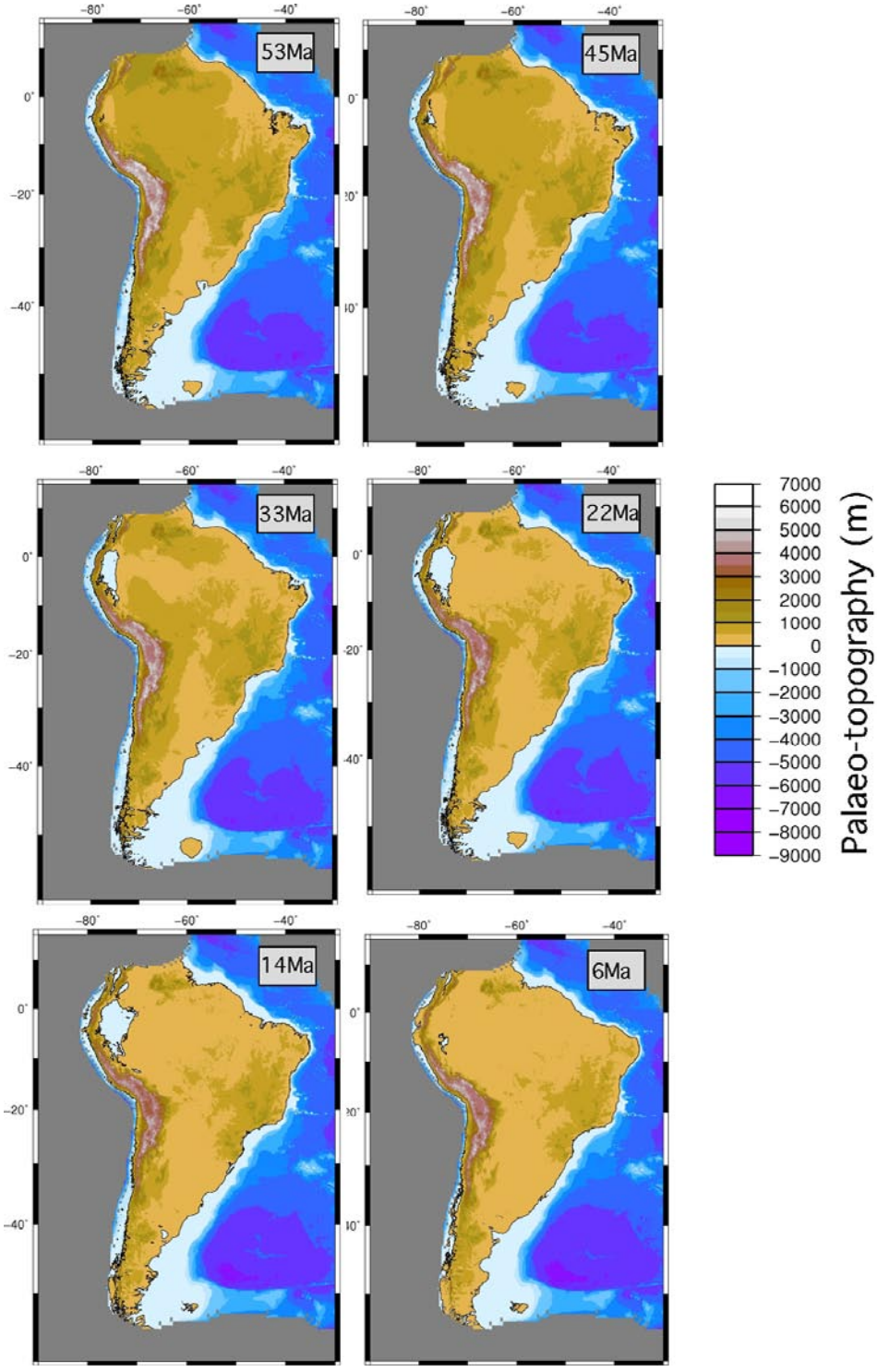

SOM Figure 5. Inundation maps of South America including palaeo-topography and predicted palaeo-coastline (black) produced using Haq *et al.* (1987) sea level curve from our best-fit model. Note that we have not removed any Andean mountain building, and therefore average topography along the western margin would have

been further reduced and inundation potentially greater in that region than what is shown here.

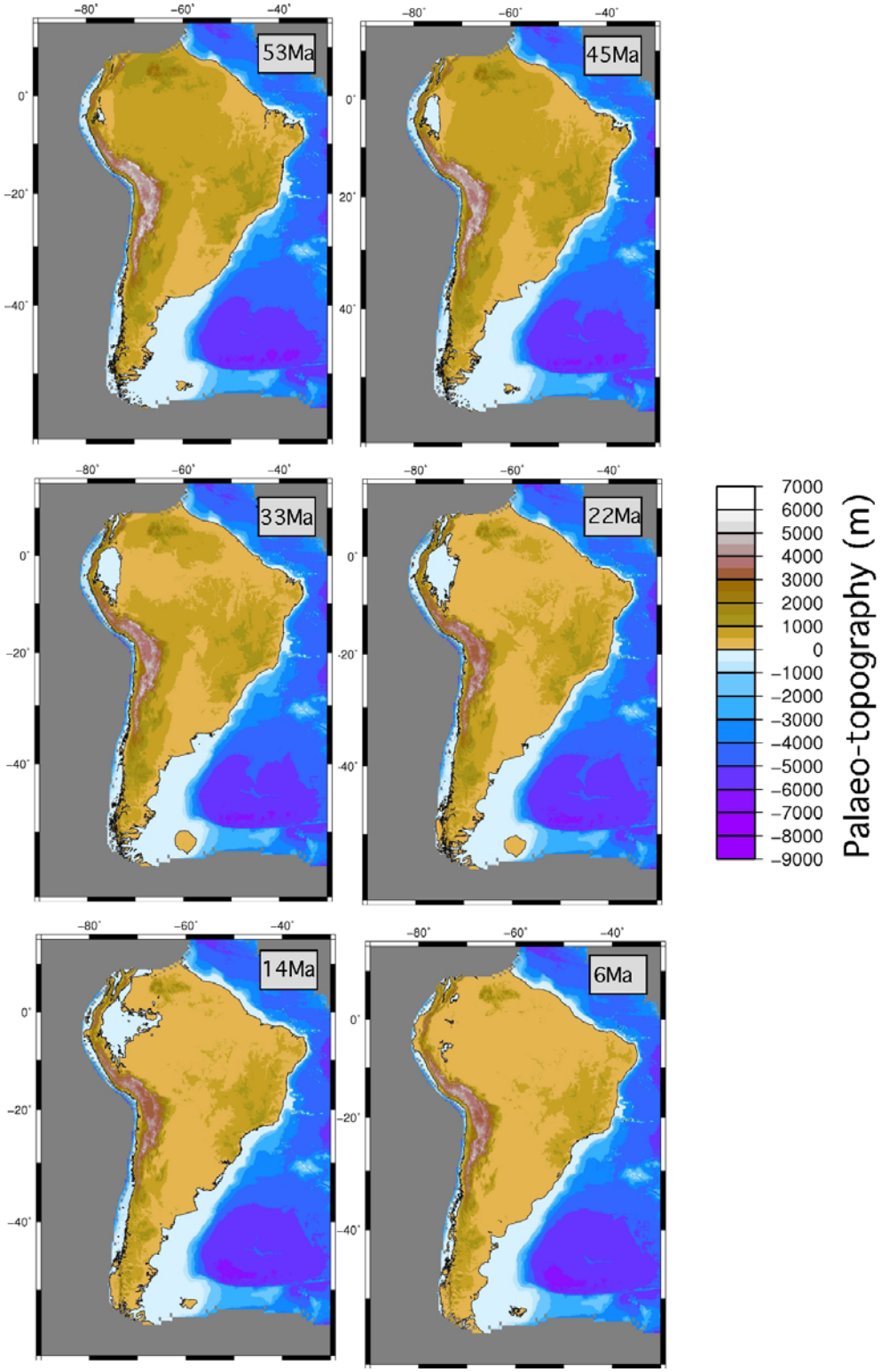

DOI: 10.1038/NGEO1017

SOM Figure 6. Inundation maps of South America including palaeo-topography and predicted palaeo-coastline (black) produced using Haq *et al.* (1987) sea level curve from the model run using a non-dimensional lower mantle viscosity of 10.

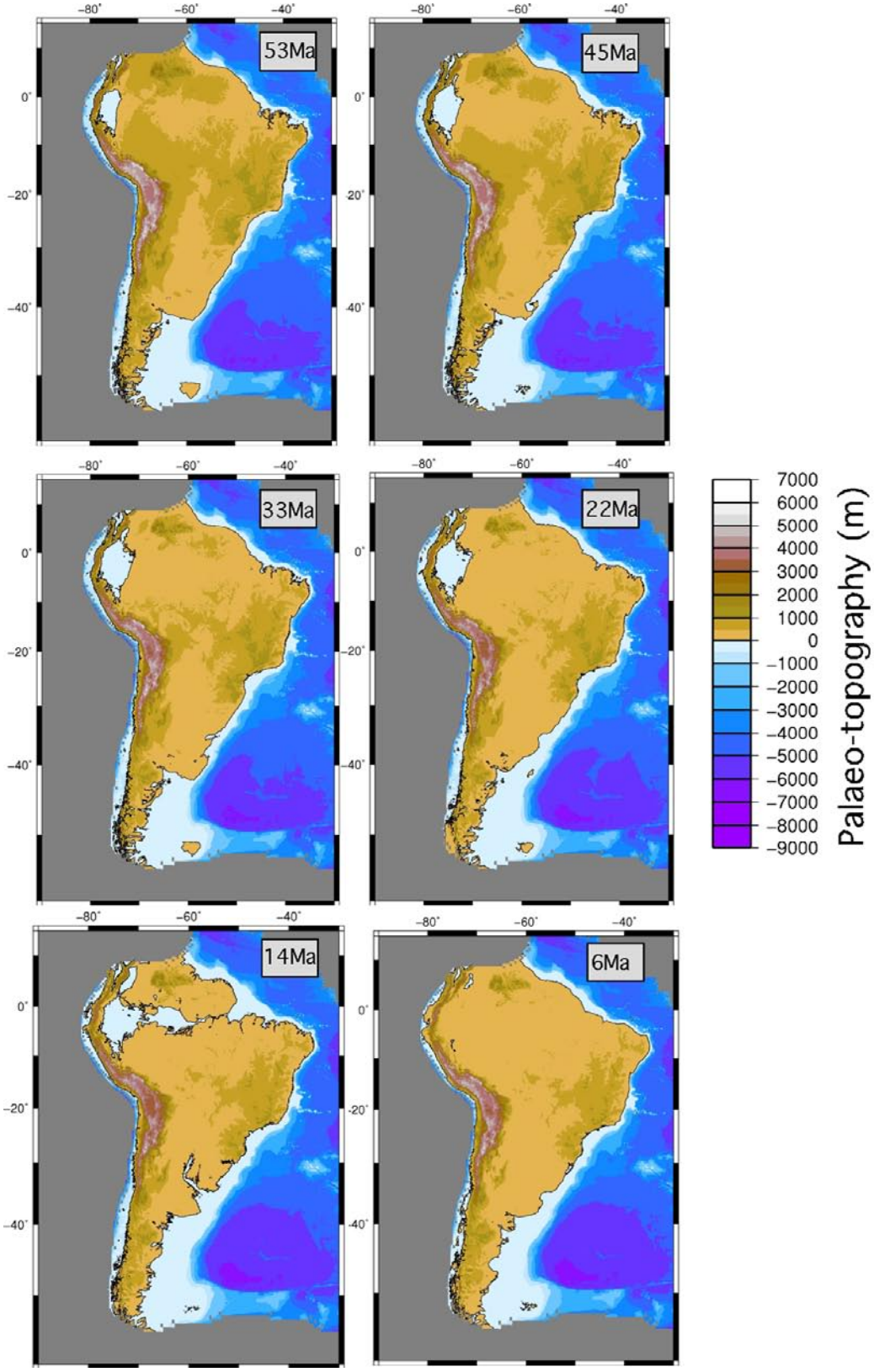

SOM Figure 7. Inundation maps of South America including palaeo-topography and predicted palaeo-coastline (black) produced using Haq *et al.* (1987) sea level curve from the model run using a non-dimensional lower mantle viscosity of 30.

DOI: 10.1038/NGEO1017

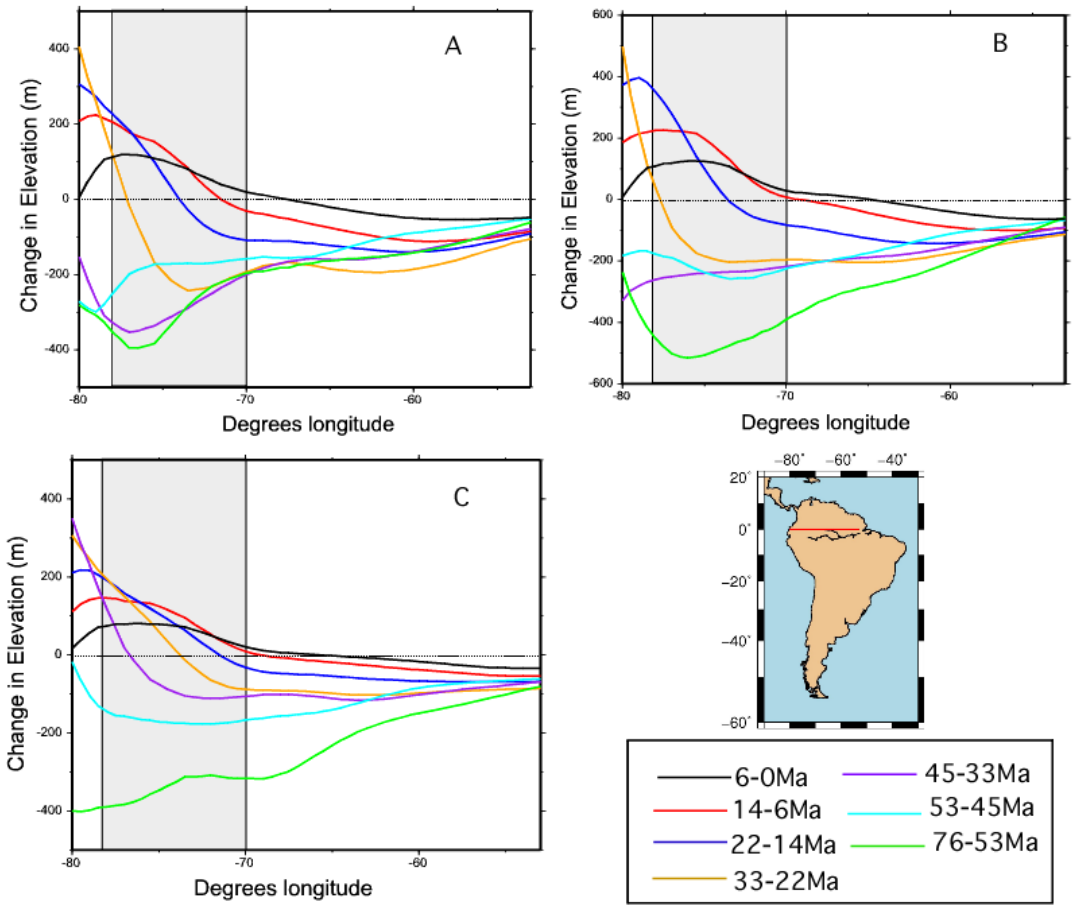

SOM Figure 8. Modelled change in continental elevation of South America at the equator for seven stages from the best-fit model (A), and non-dimensional lower mantle viscosites of 10 (B) and 30 (C). Note the eastward propagating change from subsidence to uplift in the Amazonian mega-wetland area after 33 Ma, accompanied by an accentuation of subsidence at the mouth of the evolving Amazon River. All three models show a similar temporal trend, thus showing that the variation in lower mantle viscosity has little effect on the broad-scale tilting driving the formation and disappearance of the Amazonian mega-wetland and formation of the Amazon River. Grey band indicates the approximate longitudinal extent of the Amazonian mega-wetland at this latitude (adapted from Wesselingh *et al.,* 2010).

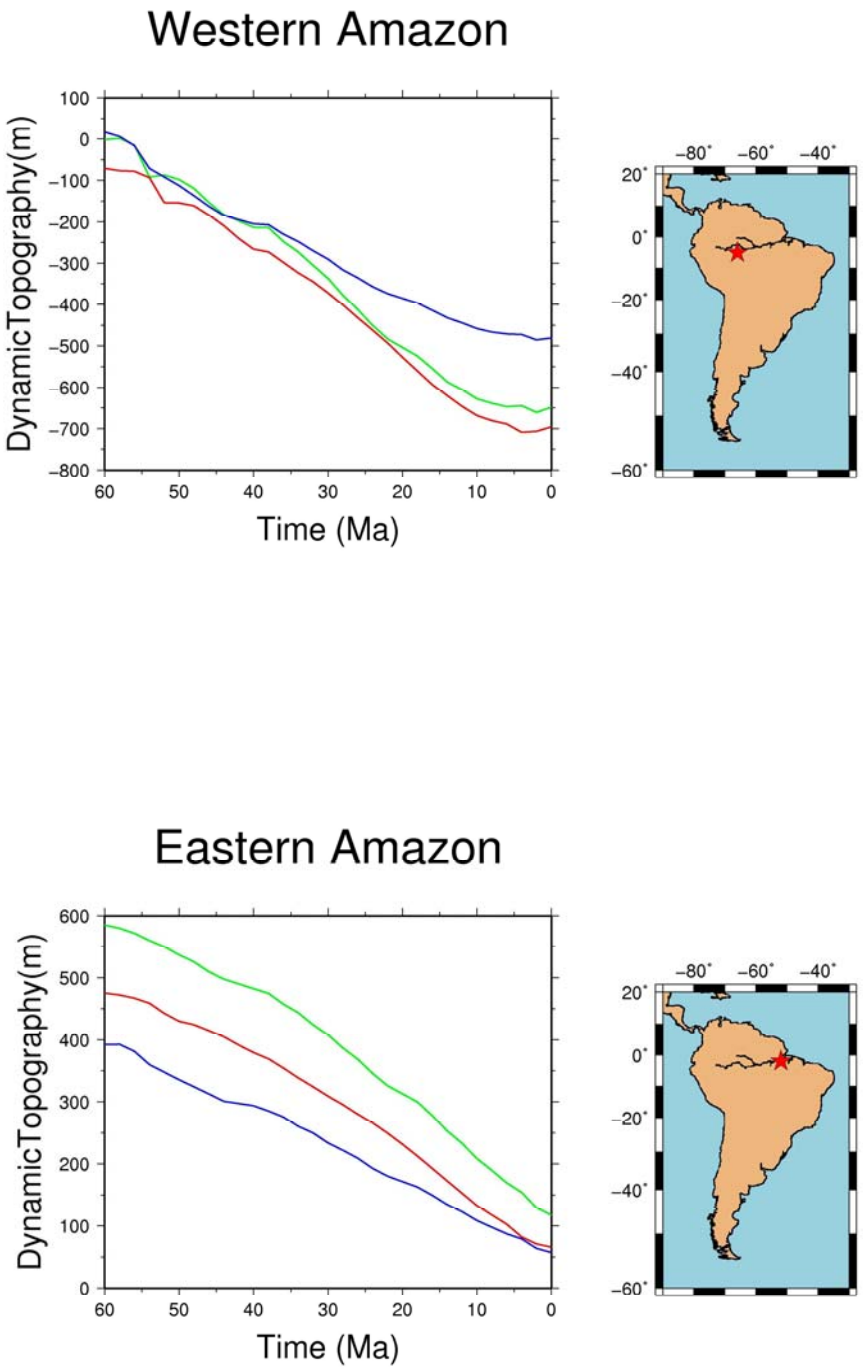

SOM Figure 9. Evolution of modelled dynamic topography within the eastern and western Amazonian sedimentary basins (see stars located on map) since 60 Ma for the three model runs. Red = Best-fit model with non-dimensional lower mantle viscosity

DOI: 10.1038/NGEO1017

of 15, Green = non-dimensional lower mantle viscosity of 10, and Blue = non-dimensional lower mantle viscosity of 30.

Supplementary Discussion

During the inverse modeling, we start with present-day mantle structure inferred from seismic tomography, and attempt to reconstruct past subduction processes. Density anomalies associated with the slab and upper and lower mantle viscosities are allowed to vary, which are then constrained by fitting the evolving continental-scale Late Cretaceous marine inundation, sediment isopachs and inferred borehole tectonic subsidence (best-fit parameters from a North America model). There is a trade-off between assumed viscosity and slab buoyancy on the inverted mantle thermal structure in the past. But different slab buoyancies predict different magnitudes of dynamic subsidence (i.e., areas of flooding), while different mantle viscosities predict different rates of change of vertical motions. These properties eventually allow separate constraining of these uncertain model parameters. In doing so, we chose a two-layer viscosity mantle to reduce the number of unknowns. From our earlier work (Liu *et al.,* 2008 and Spasojevic *et al.,* 2009), we found that the amount of data we had over North America will allow a constraint for a two-layer viscosity mantle to the best. Tests indicate that the very shallow part of mantle viscosity structure is not sensitive to this study due to the imposed plate motions. The lower mantle viscosity is the most sensitive to the large-scale evolving dynamic subsidence, while the effect of the average upper mantle viscosity is less obvious. Therefore, we provide two extra models with different lower mantle viscosity values to investigate their effects on the dynamic topography over South America.

All three models produce a similar trend of results, with broad subsidence across South America from 60 Ma, and easterly propagating uplift from the Miocene (Figs. S5 – S11). However, there are variations in the magnitude and duration of subsidence or uplift, with the greatest variability in the west of the continent. A non-dimensional lower mantle viscosity of 30 appears to produce the best-fitting inundation of the Amazonas region among all three models (Fig. S7). On the other hand, non-dimensional a lower mantle viscosity of 10 seems to overpredict the Amazonas inundation (Fig. S6). A non-dimensional viscosity of 15 (Fig S5.) was the best-fit model for South America marine inundations.

A greater viscosity of the lower mantle (the upper mantle viscosity fixed) means a smaller upper/lower mantle viscosity ratio, and this leads to a smaller present-day dynamic topography, given the same mantle density distribution (Liu and Gurnis, 2008). The differential dynamic topography during the geological past (with respect to the present), when the slabs were at shallower depth, is larger than predictions based on a smaller lower mantle viscosity, leading to more subsidence (Figs. S5, S7). However, a smaller lower mantle viscosity allows the slab to sink faster, which suggests a later subduction and more slab material beneath the overriding plate. This leads a more sustained inundation, especially toward the present day (Fig. S5, S6).

Supplementary References

Golonka, J., Krobicki, M., Pajak, J., Van Giang, N., and Zuchiewicz, W. *Global plate tectonics and paleogeography of Southeast Asia*. (Arkadia, AGH University

of Science and Technology, 128 p. 2006)

Haq, B. U. & Al-Qahtani, A. M. Phanerozoic cycles of sea-level change on the Arabian Platform. *GeoArabia* **10**, 127-160 (2005)

Haq, B.U., Hardenbol, J. & Vail, P.R. Chronology of Fluctuating Sea Levels Since the Triassic. *Science*, **235,** 1156-1167 (1987).

Liu, L., Spasojevic, S. & Gurnis, M. Reconstructing Farallon Plate Subduction Beneath North America Back to the Late Cretaceous. *Science* **322,** 934-938 (2008).

Liu, L. & Gurnis, M. Simultaneous inversion of mantle properties and initial conditions using an adjoint of mantle convection. *J. Geophys. Res.* **113** B08405 (2008).

Miller, K.G. *et al.* The phanerozoic record of global sea-level change: *Science* **310**, 1293-1298. (2005)

Müller, R.D., Sdrolias, M., Gaina, C. Steinberger, B. & Heine, C. Long-term sea-level fluctuations driven by ocean basin dynamics. *Science*. **319,** 1357-1362, (2008)

Spasojevic, S., Liu, L. & Gurnis, M. Adjoint models of mantle convection with seismic, plate motion and stratigraphic constraints: North America since the Late Cretaceous. *Geochemistry, Geophysics, Geosystems,* **10,** Q05W02 (2009)

Spasojevic, S., Liu, L., Gurnis, M. & Müller, R.D. The case for dynamic subsidence of the U.S. east coast since the Eocene. *Geophys. Res. Lett.* **35,** L08305 (2008)

Wesselingh, F. *et al.* On the origin of Amazonian landscapes and biodiversity: a synthesis, *in* Hoorn, C., and Wesselingh, F. (eds) *Amazonia: Landscape and species evolution*, (Wiley-Blackwell p.p. 421-431 2010)